

Impact properties of NIFS-HEAT-2 (V–4Cr–4Ti) after YAG laser welding and neutron irradiation at 563 K

Takuya Nagasaka ^{a,*}, Nam-Jin Heo ^{a,1}, Takeo Muroga ^a, Arata Nishimura ^a,
Hideo Watanabe ^b, Minoru Narui ^c, Kenji Shinozaki ^d

^a National Institute for Fusion Science, Oroshi, Toki, Gifu 509-5292, Japan

^b Research Institute for Applied Mechanics, Kyushu University, Kasuga 816-8580, Japan

^c Oarai Branch, Institute for Materials Research, Tohoku University, Narita, Oarai, Ibaraki 311-1313, Japan

^d Department of Mechanical System Engineering, Graduate School of Engineering, Hiroshima University, Higashi, Hiroshima 739-8527, Japan

Abstract

Weld specimens of the reference low activation vanadium alloy, NIFS-HEAT-2, were irradiated up to the neutron fluence of $4.5 \times 10^{23} \text{ nm}^{-2}$ (0.08 dpa) at 563 K in JMTR. The weld metal showed larger irradiation hardening than that of the base metal, and the weld metal showed an embrittlement at 77 K. However, irradiation hardening at the weld metal was effectively reduced by post weld heat treatment at 873 and 1223 K. Mechanisms of irradiation hardening, and behavior of C, N and O impurities in the weld metal was discussed, based on the characterization of radiation defects.

© 2004 Elsevier B.V. All rights reserved.

1. Introduction

Welds of high purity low activation vanadium alloys, such as NIFS-HEATs, has demonstrated good mechanical properties at as-welded condition [1,2]. Microstructural analyses on the weld metal showed decomposition and re-solution of Ti-(C, N, O) precipitates which immobilize the C, N and O impurities before welding [3]. The interstitial impurities are considered to interact with radiation defects, and affect mechanical properties as a result of enhanced irradiation hardening. In this study, weld samples of NIFS-HEAT-2 were irradiated at a low temperature to investigate the effect of irradiation hardening on impact properties, and to understand the characteristics of radiation defects in welded vanadium alloys.

2. Experimental procedure

The weld material was 4-mm-thick plates of NIFS-HEAT-2 (V–4Cr–4Ti) annealed at 1273 K for 2 h. The weld samples were made by bead-on-plate welding with 1.6 kW YAG laser in a high purity Ar. The detail of welding system has been described elsewhere [2]. Input power and welding speed were 290 J/m and 0.33 m/min, respectively. Table 1 shows concentration of C/N/O before and after welding. No significant contamination by welding was observed.

Miniature V-notch impact specimens ($1.5 \times 1.5 \times 20$ mm) were machined from the center of the plate thickness. The notch was 0.3 mm in depth and it was placed on the base metal and at the center of the weld metal, so that the crack propagates along the welding direction. The impact specimens were annealed at 673 K for 1 h for degassing hydrogen introduced during the machining and grinding. The impact properties of the degassed samples, however, was almost the same as machined (as-welded) ones [4]. Coupons with $1 \times 4 \times 20$ mm in size and TEM (Transmission electron microscope) disks with $\phi 3 \times 0.25$ mm were also prepared for hardness test

* Corresponding author. Tel.: +81-572 58 2252; fax: +81-572 58 2676.

E-mail address: nagasaka@nifs.ac.jp (T. Nagasaka).

¹ Present address: Center for Advanced Research of Energy Technology, Hokkaido University, Sapporo 060-8628, Japan.

Table 1
Impurity levels of NIFS-HEAT-2 before and after YAG laser welding in high purity Ar (wppm)

	Cr*	Ti*	H	C	N	O
Before	4.00	4.02	29	51	123	139
After			35	49	129	158

around the bead and microstructural observation, respectively. In order to investigate the effect of post weld heat treatment (PWHT), the coupons and the TEM disks were annealed for 1 h at 673, 873 and 1223 K. The samples were irradiated in JMTR (Japan Materials Testing Reactor) at 563 K. The neutron fluence was $4.5 \times 10^{23} \text{ nm}^{-2}$ (0.08 dpa).

3. Results

Fig. 1 shows the results of Charpy impact test. Absorbed energy is normalized by the function of ligament size, which is $B \times b = 1.5 \times 1.2 \text{ mm}^2$. Before irradiation, both the base metal (BM) and the weld metal (WM) maintained good ductility at all test temperatures. Upper shelf energy, E_U , was estimated as 0.4 J m^{-3} . After irradiation, upper shelf energy of the base metal and weld metal was around 0.35 J m^{-3} , which was 10–15% lower than that before irradiation. In addition, absorbed energy of the weld metal after irradiation showed a remarkable drop at 77 K. Ductile-brittle transition temperature (DBTT) of the weld metal after irradiation was estimated as 113 K, where absorbed energy was expected to be half the upper shelf energy before irradiation. DBTTs for the other curves were less than 77 K. Fig. 2 shows the scanning electron microscope images of fracture surface at 77 K for irradiated specimens. In contrast to 16% of the cleavage fracture area for the base metal, 85% of the fracture surface was cleavage for the weld metal. The figure also indicates plastic deformation

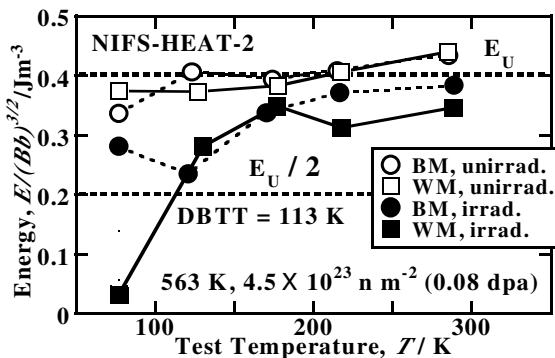


Fig. 1. Test temperature dependence of absorbed energy at Charpy impact test before and after the neutron irradiation.

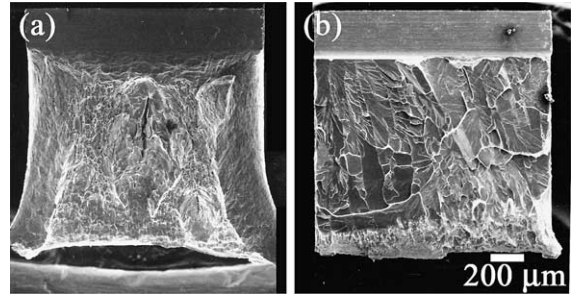


Fig. 2. Fracture surface of (a) the base metal and (b) the weld metal at 77 K after irradiation.

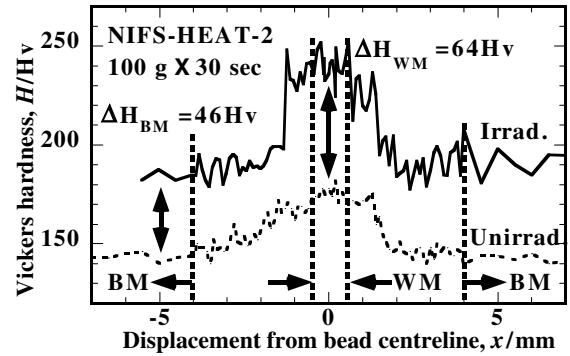


Fig. 3. Hardness distribution around the bead. The vertical dashed lines indicate regions of the weld metal and the base metal. Irradiation hardening, ΔH , was the difference of the average hardness of the regions.

during Charpy test was much lower for the weld metal compared with that for the base metal.

Fig. 3 shows hardness distribution around the bead. From microstructural observations, the width of the weld metal was 1 mm as indicated in the figure. Base metal regions were determined as 4 mm or farther from the bead center, where the hardness before irradiation was the same as that before welding. Irradiation hardening was estimated as the difference between the average hardness in each regions. Irradiation hardening of the weld metal, 64 Hv, was 40% larger than that of the base metal, 46 Hv. Fig. 4 shows the effect of PWHT on irradiation hardening. Hardness of the base metal was independent of PWHT either before or after irradiation. On the other hand, hardness of irradiated weld metal was effectively reduced by PWHT. Irradiation hardening of the weld metal after PWHT at 873 and 1223 K was similar to that of the base metal.

Fig. 5 shows TEM images of radiation defect structure in the base metal and the weld metal with various PWHT. The defect structures were very similar to each other, and consisted of black dots. From analyses on their characteristics, the dots are identified to be small

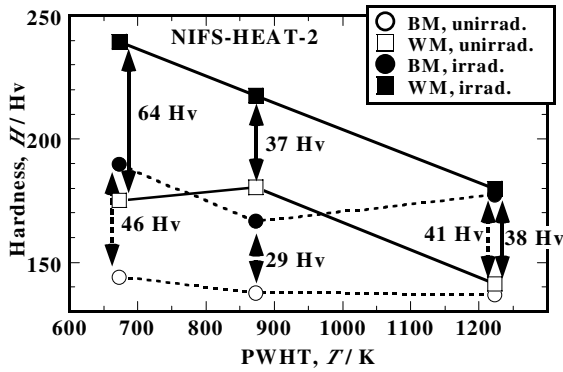


Fig. 4. Effect of PWHT on hardness of the base metal and the weld metal. The arrows and hardness number indicate irradiation hardening after PWHT.

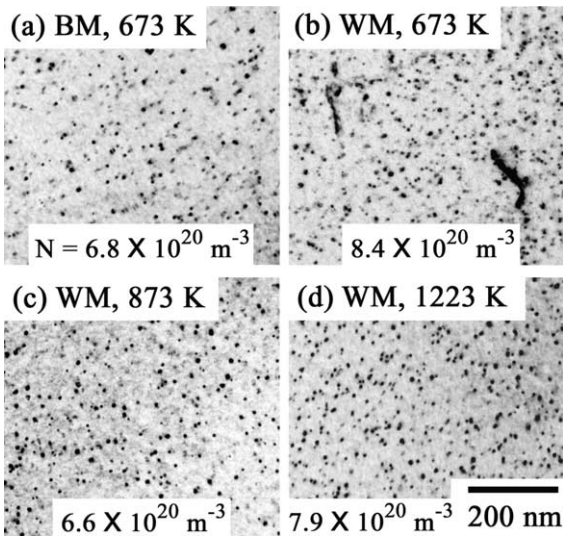


Fig. 5. TEM images of radiation defects structure in the base metal and weld metal with various PWHT. N is the number density of the black dots.

dislocation loops with a Burger's vector of $1/2\langle 111 \rangle$ or $\langle 100 \rangle$.

4. Discussion

4.1. Embrittlement of the weld metal at 77 K

The weld metal became brittle at 77 K after irradiation as shown in Fig. 1. However, no responsible defect was observed on the fracture surface as shown in Fig. 2. The weld metal showed less plastic deformation. Thus, it is recognized that the large hardening shown in Fig. 4 is responsible for the embrittlement of the weld metal at 77 K. Yield stress is considered to be raised by irradiation

hardening, and be higher than the stress for cleavage fracture. Suppression of irradiation hardening at weld metal will be effective to avoid the embrittlement.

4.2. Hardening mechanism at weld metal

Radiation defects as dislocation loops observed in Fig. 5 can induce hardening. The loop number density of the weld metal after irradiation (WM, 673 K) was larger than that of the base metal (BM, 673 K). Orowan's equations describing the relationship between dislocation loop barriers and hardening can be written as [5],

$$\Delta H_{M-T} = \alpha_H \mu b \sqrt{N_{M-T} d}, \quad (1)$$

ΔH : irradiation hardening, M : material, BM or WM, T : PWHT, α_H : barrier strength converted for hardness by assuming that shear stress for dislocation migration is proportional to hardness, μ : shear modulus, b : Burger's vector, N : number density of dislocation loops, d : diameter of dislocation loops.

Assuming that α_H and d is constant because the defect structures were quite similar to each other, the ratio of irradiation hardening can be predicted from the loop number densities as follows:

$$\Delta H_{WM-673K} = \alpha_H \mu b \sqrt{N_{WM-673K} d}, \quad (2)$$

$$\Delta H_{BM-673K} = \alpha_H \mu b \sqrt{N_{BM-673K} d}, \quad (3)$$

(2) and (3) are merged, then the number densities in Fig. 5 are substituted,

$$\frac{\Delta H_{WM-673K}}{\Delta H_{BM-673K}} = \frac{\sqrt{N_{WM-673K}}}{\sqrt{N_{BM-673K}}} = \frac{\sqrt{6.8 \times 10^{20}}}{\sqrt{8.4 \times 10^{20}}} = 1.1. \quad (4)$$

The dislocation loop density can only explain 10% of additional hardening in the weld metal, while the real hardening of the weld metal was 40% larger than that of the base metal.

From a study on pure vanadium, the present authors have reported that nitrogen enhanced cold-work-anneal hardening and radiation-anneal hardening (RAH) at 573 K [6]. In pure vanadium, all the nitrogen was recognized to be at interstitial position because of no precipitation microstructure. Threshold concentration of nitrogen for the anneal hardenings was 100–200 wppm. Oxygen has no effect on the anneal hardenings. In the weld metal, most of the 129-wppm nitrogen is considered to be at interstitial position, and they can migrate below 563 K. Moreover, radiation defects may enhance the mobility of the other interstitial impurities, such as carbon and oxygen. The impurities are thought to decorate and stabilize the dislocation loops. Therefore the barrier strength, α_H , could be increased during irradiation. On the other hand, Ti-(C, N, O) precipitates appeared in the base metal and also in the weld metal of

gus-tungsten-arc weld after PWHT at 973–1223 K [4]. Recently, it has been reported that the precipitation was started at 873 K for YAG laser weld [7]. After PWHT at 873 and 1123 K, most of the interstitial impurities were thought to be already disappeared by precipitation, and could not migrate to decorate the dislocation loops during irradiation. By replacement of α_H in Eq. (2) into the enhanced barrier strength, α'_H ,

$$\Delta H_{WM-673 K} = \alpha'_H \mu b \sqrt{N_{WM-673 K} d}, \quad (5)$$

$$\Delta H_{BM-673 K} = \alpha_H \mu b \sqrt{N_{BM-673 K} d}, \quad (6)$$

$$\frac{\alpha'H}{\alpha H} = \frac{\Delta H_{WM-673 K}}{\Delta H_{BM-673 K}} \frac{\sqrt{N_{BM-673 K}}}{\sqrt{N_{WM-673 K}}} = \frac{64 \sqrt{8.4 \times 10^{20}}}{46 \sqrt{6.8 \times 10^{20}}} = 1.253. \quad (7)$$

For the anneal hardenings in the pure vanadium, the ratios of barrier strength were 1.35. The above result is much closer to the experimental results than that in the case of constant α_H .

4.3. Optimum PWHT to improve the performance of weld joint

Fig. 6 shows comparison of irradiation hardening to other low activation vanadium alloys, such as US832665, a large heat by US-DOE [8], and VM9401 [9], by a laboratory scale melting. Only the data on the plate before welding, which is equivalent to base metal, are available for the two alloys. Irradiation hardening of the base metal of NIFS-HEAT-2 was the lowest among the alloys. Moreover, irradiation hardening of the weld metal was still comparable to the other alloys. Thus, NIFS-HEAT weld joints are expected to show better

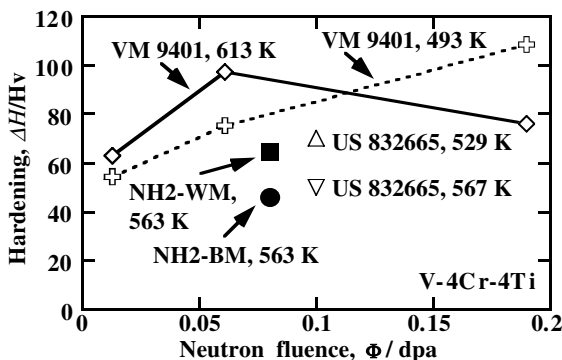


Fig. 6. Neutron fluence dependence of irradiation hardening of three V-4Cr-4Ti alloys, such as NIFS-HEAT-2 (NH2), US832665 [8] and VM9401 [9]. Concentrations of C/N/O in US832665 are 80/85/310 wppm, respectively. N/O in VM9401 are 6/240 wppm.

impact properties than the other alloys. Possible cause for the lower irradiation hardening at NIFS-HEAT is the oxygen level which is almost half that in the other alloys. Systematic study on the behavior of the each interstitial impurities is necessary to obtain a future principle for impurity control.

Fig. 4 indicates that a PWHT higher than 873 K will likely be effective. Another work has reported that long term annealing at 873 K induced large precipitation hardening and embrittlement [7]. It was also shown that after annealing at 1223 K, coarsening of Ti-(C, N, O) precipitates degraded impact properties, in spite of hardness recovery in the weld metal [7]. The optimum PWHT temperature for NIFS-HEAT should be between 873 and 1223 K, where suitable precipitation size and distribution are expected without causing precipitation hardening, over-coarsening of precipitates or irradiation hardening. It has been preliminarily reported that the weld metal of NIFS-HEAT-2 after annealing at 1073 K indicated small hardening and lower DBTT than 150 K [7].

5. Conclusions

Weld specimens of the reference low activation vanadium alloy, NIFS-HEAT-2, was irradiated up to $4.5 \times 10^{23} \text{ nm}^{-2}$ (0.08 dpa) in neutron fluence by using JMTR at 563 K. Effect of irradiation hardening on impact properties and characteristics of radiation defects produced in the weld were investigated.

- (1) The weld metal showed larger irradiation hardening than that of the base metal. The weld metal showed an embrittlement at 77 K after neutron irradiation. DBTT was raised up to 113 K for the irradiated weld metal.
- (2) Irradiation hardening at the weld metal was effectively reduced by post weld heat treatment at 873 and 1223 K.
- (3) Radiation defects in the weld metal were identified as dislocation loops. The number density and the size of them were quite similar to those in the base metal. PWHT did not affect the radiation defect structures.
- (4) The large irradiation hardening could be attributed to decoration and stabilization of the dislocation loops with interstitial impurities from solid solution state, which is introduced by the decomposition of Ti-(C, N, O) precipitates during welding.
- (5) Optimum PWHT temperature for NIFS-HEAT should be placed between 873 and 1223 K, where suitable precipitation size and distribution are expected without causing precipitation hardening, over-coarsening of precipitates or irradiation hardening.

Acknowledgements

This study was supported by JUPITER-II program (Japan–USA Program of Irradiation Test for Fusion Research), and the inter-university cooperative research program of the Irradiation Experimental Facility, Institute for Materials Research, Tohoku University.

References

- [1] T. Nagasaka, M.L. Grossbeck, T. Muroga, J.F. King, *Fusion Technol.* 39 (2001) 664.
- [2] N.J. Heo, T. Nagasaka, T. Muroga, A. Nishimura, K. Shinozaki, H. Watanabe, *Fusion Sci. Technol.* 44 (2003) 470.
- [3] N.J. Heo, T. Nagasaka, T. Muroga, H. Matsui, *J. Nucl. Mater.* 307–311 (2002) 620.
- [4] T. Nagasaka, T. Muroga, M.L. Grossbeck, T. Yamamoto, *J. Nucl. Mater.* 307–311 (2002) 1595.
- [5] A.L. Bement Jr., *Am. Soc. Metals* 2 (1970) 693.
- [6] T. Nagasaka, H. Takahashi, T. Muroga, N. Yoshida, T. Tanabe, *ASTM STP 1405* (2001) 746.
- [7] T. Nagasaka, N.J. Heo, T. Muroga, A. Nishimura, H. Watanabe, K. Shinozaki, 2003 Fall Meeting of the Atomic Energy Society of Japan, 24–26 September 2003, Shizuoka University, Japan.
- [8] L.L. Snead, S.J. Zinkle, D.J. Alexander, A.F. Rowcliffe, J.P. Robertson, W.S. Eartherly, *Fusion Reactor Mater.*, DOE/ER-0313/23 (1997) 81.
- [9] K.-i. Fukumoto, H. Matsui, Y. Candra, K. Takahashi, H. Sasanuma, S. Nagata, K. Takahiro, *J. Nucl. Mater.* 283–287 (2000) 535.